

# Improvement of the accuracy of radioactivity analysis using gamma spectroscopy by reducing the Compton continuum of $^{40}\text{K}$ gamma spectrum

T.Y.H. Huynh<sup>1,2</sup>, H.N.T. Truong<sup>1,2</sup>, H.L. Trinh<sup>2,3</sup>, V.T. Nguyen<sup>1,2,3\*</sup>, C.H. Le<sup>1,2</sup>

<sup>1</sup>Nuclear Technique Laboratory, University of Science, Ho Chi Minh City, Vietnam

<sup>2</sup>Vietnam National University, Ho Chi Minh City, Vietnam

<sup>3</sup>Faculty of Physics and Engineering Physics, University of Science, Ho Chi Minh City, Vietnam

## ABSTRACT

### ► Original article

#### \*Corresponding author:

V. T. Nguyen

E-mail: nvthang@hcmus.edu.vn

Received: June 2023

Final revised: January 2024

Accepted: January 2024

Int. J. Radiat. Res., July 2024;  
22(3): 565-572

DOI: 10.61186/ijrr.22.3.565

**Keywords:** Chemical separation, Compton continuum, minimum detection activity, gamma spectrum

**Background:** During the analysis of certain natural radionuclides in plant samples using gamma spectroscopy, the presence of  $^{40}\text{K}$  in the sample causes the overlap of its Compton region with the full energy peaks of  $^{238}\text{U}$ ,  $^{232}\text{Th}$ , and their daughter. Therefore, it is necessary to remove potassium before the measurement to enhance analytical accuracy. **Materials and Methods:** Five different plant samples were used to validate the method. For each sample, the analysis was performed using two separation methods (original and K-separation), and both were measured with the gamma detector. Comparison of the results achieved using the two methods with regard to spectrum, peak-to-total ratio, obtained activity, and minimum detectable activity (MDA) indicated that the proposed method yielded improved results. **Results:** The separation procedure removed most of potassium present in the samples. The peak-to-total of energy peaks < 1000 keV increased significantly. The spectrum after K-separation exhibited a lower continuum under the peaks, and the shapes of the peaks were more identifiable. Comparison of MDA values derived before and after the application of K-separation showed an improvement in analytical accuracy. **Conclusion:** The removal of potassium from plant samples is effective in decreasing the MDA of the spectroscopy by reducing the Compton continuum of the  $^{40}\text{K}$  isotope under the energy peaks of interest. Therefore, the application of this method can augment the measurement possibilities for samples with low radioactivity.

## INTRODUCTION

Plants naturally contain radioactive isotopes, including  $^{40}\text{K}$ ,  $^{238}\text{U}$  series,  $^{232}\text{Th}$  series, and  $^{235}\text{U}$  series, which emit gamma rays during alpha or beta decay. Gamma spectroscopy using high-purity germanium (HPGe) detectors or scintillation detectors (e.g., NaI (Tl)) are commonly employed to analyze the radioactivity of plants <sup>(1)</sup>. The method includes several continuous stages, such as sample preparation, measurement, and spectrum analysis. For this purpose, gamma spectroscopy is preferred because of the low background, appropriate energy resolution, and low minimum detectable activity (MDA) <sup>(2)</sup>. During gamma spectrum analysis of low-activity samples, such as plant samples, differentiating between signals from the energy of the peak of interest and those from the background can be challenging <sup>(3)</sup>. The low activity concentration of the radioisotope is related to a low radiation level, and it is difficult to distinguish between the signals from the considered energy and those from background radiation in the environment. The

following techniques can be employed to optimize the measurement conditions and improve the detection sensitivity and accuracy of measuring low-activity plant samples using gamma spectrometry: (1) Shielding: The use of appropriate shielding materials, such as lead or copper, can reduce background radiation and minimize interference. (2) Background subtraction: By measuring and characterizing the background radiation separately, it can be subtracted from the sample measurements to isolate the specific signals of interest <sup>(4)</sup>. (3) Extension of the counting time: The long counting time applied for the analysis allows the accumulation of more data, which can improve the signal-to-noise ratio and help differentiate the sample signal from the background. (4) Energy window selection: Setting specific energy windows for the gamma spectrometer can aid in focusing on the desired energy range emitted by the radioactive isotopes, effectively reducing the impact of unrelated background radiation <sup>(5)</sup>. (6) Quality control: Regular calibration and monitoring of the gamma spectrometer and performing blank measurements can help identify and address any

instrumental noise or background contamination issues (6).

Enhancing the accuracy and sensitivity of the measurements of radioisotopes in low-level radioactive samples is a research topic that has attracted immense attention (7-9). In analyses using the gamma spectrometer, distinguishing the energy peaks of radioisotopes from background radiation emanating from environmental radionuclides and unconsidered radionuclides in the sample is difficult (3,5). As discussed above, one of the methods to solve this problem is increasing the mass of the sample. Normally, a large volume of the plant sample is collected and burned in the furnace to reduce its sample size so that it is suitable for analysis (10). In environmental studies, popular natural radionuclides, such as  $^{232}\text{Th}$ ,  $^{226}\text{Ra}$ ,  $^{238}\text{U}$ , and  $^{40}\text{K}$ , have been focused on. Generally, the radioisotope present at the highest concentration in natural soil and plant samples is  $^{40}\text{K}$  (11-13). Thus, the Compton continuum of  $^{40}\text{K}$  contributes majorly to the gamma spectrum of the sample. The  $^{238}\text{U}$  activity is determined using the gamma energy peaks at 63.3 keV and 92.6 keV of  $^{234}\text{Th}$ ,  $^{232}\text{Th}$  activity with the peaks at 338.3 keV and 911.1 keV of  $^{228}\text{Ac}$ , and  $^{40}\text{K}$  with its energy peak at 1,461 keV. When the activity of the  $^{40}\text{K}$  isotope is much higher than that of others, the Compton region of the  $^{40}\text{K}$  spectrum can cause an increase in the counts of the energy between 50 keV and 1220 keV. This increase affects the accuracy of the analytical results, especially for  $^{238}\text{U}$  whose peaks are at 63.3 keV and 92.6 keV. Therefore, to improve the accuracy of the radioactivity analysis of plant samples,  $^{40}\text{K}$  was removed using chemical methods. Furthermore, the influence of the Compton region of  $^{40}\text{K}$  on the energy peaks of the other isotopes was evaluated.

Several methods have been applied to reduce background radiation in gamma spectroscopy for enhancing the accuracy of radioactivity analysis. The most popular method is shielding strengthening to reduce background radiation, such as those from environmental radionuclides, radon gas, and cosmic rays (14,15). The Monte Carlo method is also applied to minimize the impact of this effect on sample gamma spectrums (16-19). The removal of potassium from the measurement samples to improve the efficiency of gamma spectrum analysis is not popular. Biota samples normally have high radioactivity of  $^{40}\text{K}$  but very low radioactivity of uranium and thorium series. Therefore, it is necessary to apply this method for radiation measurements in this sample type.

## MATERIALS AND METHODS

### Sample collection and preparation

Plant samples were collected from the suburban region of Ho Chi Minh City, Vietnam (coordinates:  $10^{\circ}$

$52'33.3''$  N and  $106^{\circ}47'26.4''$  E) in December 2021. Leaf samples from aloe vera (*Aloe vera* var. *chinensis*), spruce (*Picea abies*), vetiver grass (*Chrysopogon zizanioides* L), red amaranth (*Amaranthus cruentus* L), and water spinach (*Ipomoea aquatica*) were assigned the names VERA, PINE, VERT, AMAR, and SPIN, respectively. The map of the sample location is shown in figure 1.

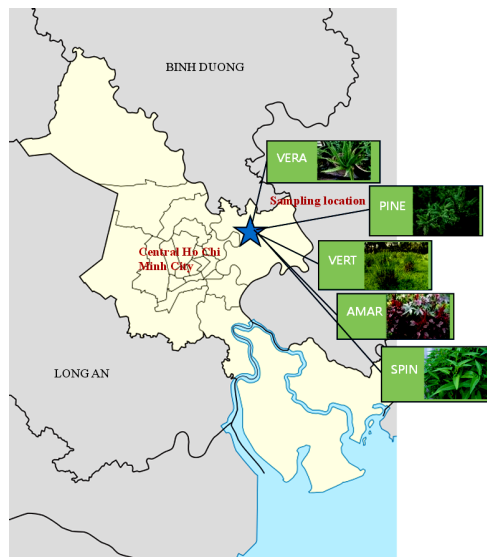


**Figure 1.** Map of Ho Chi Minh City showing the sample location in the insert.

The procedure for sample preparation and analysis using gamma spectroscopy followed the standard procedure (10). At the laboratory, the samples were desiccated in a drying cabinet to remove the water content. The samples were then ashed in a furnace (Mettler GmbH) at  $450^{\circ}\text{C}$  for 1 day to reduce the volume and remove the organic matter. The ash was ground into a powder form and sieved to collect particles with a diameter of  $< 200\ \mu\text{m}$ . Each sample was packed, sealed, and labeled in a cylindrical container made from nonradioactive material and was subsequently stored for 30 days at room temperature before the measurement. As the plant samples exhibited low radioactivity, they had to be measured for a long time (approximately 86,400 s) to reduce statistical uncertainty.

### Radioactivity analysis

To analyze the activity concentrations of natural radionuclides, the procedure used in several previous studies was adopted (20-22). The gamma spectrometer manufactured by ORTEC was employed to determine the anthropogenic and natural radioactivity in the samples. The instrument was equipped with a n-type HPGe detector (GMX35P4-70) cooled using X-Cooler III. The relative detector efficiency was 35%, and the gamma-ray energy resolution was 1.8 keV at 1.33 MeV, which was calibrated with a standard point source. The detector was placed inside a 10 - cm thick lead shield.

Energy window analysis (EWA) is a technique routinely employed for gamma spectrum analysis using gamma spectroscopy <sup>(23)</sup>. This method enhances the detection limit for the analysis of specific radionuclides or energy regions of interest while minimizing the influence of background radiation. EWA involves setting specific energy windows or regions within the gamma-ray spectrum to isolate and analyze the desired radionuclides or gamma-ray emissions. Activity concentrations of radioisotopes derived at their gamma-ray energies were calculated using Eq (1).

$$A = \frac{S}{\varepsilon(E) \times m \times f \times t \times K_c \times K_w} \quad (1)$$

Where, A is the activity concentration of the sample (Bq kg<sup>-1</sup>), S is the net peak area (count),  $\varepsilon(E)$  is the attenuation detection efficiency at the peak energy, m is the mass of the sample (kg), f is the branching ratio of the gamma energy E under consideration, t is the counting live time (s),  $K_c$  is the correction factor for the nuclide decay during the counting, and  $K_w$  is the correction factor for radioactive decay from the time of sample collection to the point of spectroscopic measurement <sup>(5)</sup>.

For gamma analysis, the detection efficiency varies for different gamma energy levels. Moreover, the efficiency depends on the characteristics of the detector used, background, and sample geometry and matrix. Therefore, it must be corrected to assure the accuracy of the measurement. In this study, the full energy peak efficiency of the detector was calibrated using the Angle 3.0 software supported by ORTEC. The peak efficiency for a given sample geometry and composition was based on the experimental efficiencies for the geometry and composition of the standard sample determined using effective solid angle calculations.

For gamma spectrum analysis, the accuracy of the analytical method was assessed using the minimum radioactivity of the radioisotope that can be spectroscopically detected. This is also known as the MDA and is defined by the Currie MDA algorithm in Eqs (2) and (3) <sup>(5)</sup>.

$$MDA = \frac{L_D}{\varepsilon(E) \times m \times f \times t \times K_c \times K_w} \quad (2)$$

$$L_D = 2.71 + 3.29 \sqrt{2B + \left(\frac{T_s}{T_b}\right) I + \left(\frac{T_s}{T_b}\right)^2 \sigma_I^2} \quad (3)$$

Where,  $L_D$  is the detection limit for the confidence interval of 95%, I is the net peak area of the background measurement,  $\sigma_I$  is the standard deviation of I, B is the value of the continuum under the peak,  $T_s$  is the live time of the sample measurement, and  $T_b$  is the live time of the background measurement <sup>(5)</sup>.

The obtained activity value is acceptable only if it

is greater than the MDA value for a specific sample type. An activity value that is lower than the MDA value indicates that the measured concentration of the isotope is near or below the sensitivity of the instrument or the detection limit of the analytical method. In such cases, it becomes challenging to improve the accuracy of the measurements or draw meaningful conclusions about the actual activity levels of the isotopes in the samples.

Noting the activity value that is lower than the MDA is important. This observation does not mean that the activity is zero or that radioisotopes are not present in the samples. It merely indicates that the measurement technique or the instrument used may not have sufficient sensitivity to detect the activity that is below the reported MDA. Thus, to enhance the accuracy of radioactivity analysis, MDA should be reduced to the maximum possible extent. One way to reduce the MDA is to decrease the background radiation, which means lowering the continuum under the energy peak.

### Potassium extraction

To extract potassium from the samples, after the measurement using gamma spectroscopy, the ash samples were stirred at 300 rpm in 1000 mL of 1 M amino acetate solution to dissolve the potassium. After 1 h, the sample solution was filtered through a paper filter to remove the potassium from the ash samples. The analytical reagents were supplied by Sigma-Aldrich. The obtained solid was then dried in an oven at 80°C for 48 h until the sample was completely dry. The samples VERA, PINE, VERT, AMAR, and SPIN were again sieved, packed, sealed, and labeled in containers denoted as TK-VERA, TK-PINE, TK-VERT, TK-AMAR, and TK-SPIN, respectively. These measurement and analysis procedures were repeated to determine the activity concentration of radioisotopes.

### Statistical analysis

The experimental data were analyzed, and the charts were drawn using Microsoft Excel. All data were found to be normally distributed ( $p < 0.05$ ) at a confidence interval of 95%. The MAESTRO Multichannel Analyzer Emulation Software of ORTEC was used for gamma spectrum analysis.

## RESULTS

The influence of <sup>40</sup>K on the energy peaks of other isotopes in ashed plant samples was evaluated by analyzing the obtained spectrums before and after the separation of potassium. Spectrums of the samples with an energy range of 0–1500 keV (the energy peak of <sup>40</sup>K is at 1460 keV) before and after K-separation are presented in figure 2 To strictly observe the <sup>40</sup>K Compton continuum on the energy peaks of other isotopes, the spectrums were

categorized into three distinct regions of 0–500 keV, 500–1000 keV, and 1000–1500 keV. For example, the spectrums of the vetiver grass sample are shown in figure 2 in the figure, the legend “VERT” denotes the gamma spectrum of the vetiver grass sample before the K-separation and “TK-VERT” signifies the gamma spectrum of the sample after the application of K-separation. The graphs demonstrated that the Compton continuums of TK-VERT spectrums were lower than the corresponding continuums of VERT spectrums, especially for the energy range of 0–500

keV. This is the region containing the energy peaks used for the activity analysis of most natural radionuclides.

To better understand the differences between the spectrums before and after K-separation in the energy range of 0–100 keV, the comparison is shown in figure 3 the graphs suggested that the application of K-separation significantly reduced the Compton continuum. Similar results were obtained for the spectrums of VERA, VERT, AMAR, and SPIN samples.

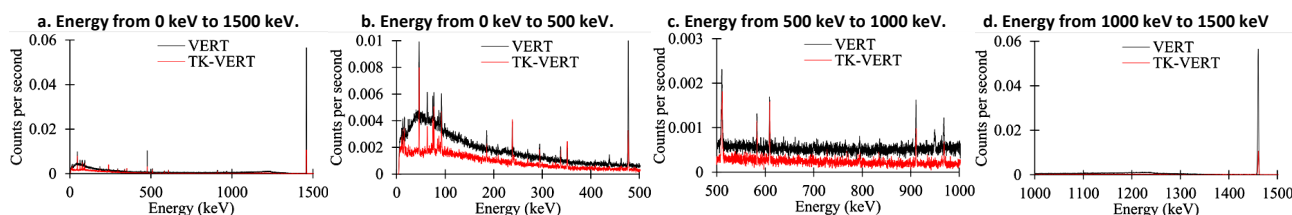


**Figure 2.** Gamma spectrums of the vetiver grass sample before and after K-separation: (a) energy range 0–1500 keV, (b) energy range 0–500 keV, (c) energy range 500–1000 keV, and (d) energy range 1000–1500 keV.

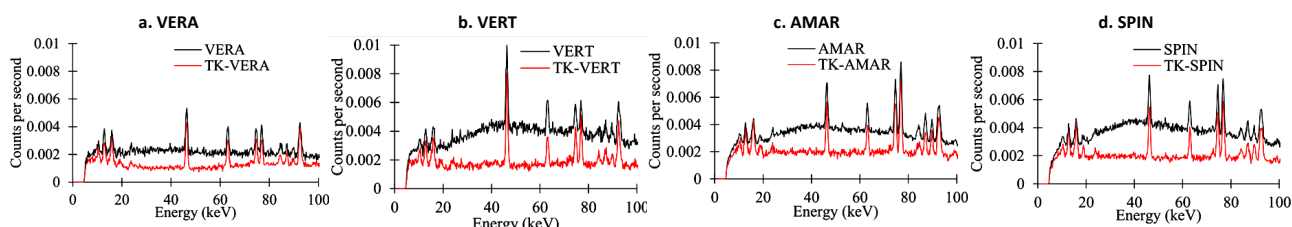


**Figure 3.** Spectrums of the different samples before (sample IDs: VERA, VERT, AMAR, SPIN) and after (sample IDs: TK-VERA, TK-VERT, TK-AMAR, TK-SPIN) K-separation at the energy of < 100 keV.

Figure 3 demonstrated a significant reduction in the Compton continuum of spectrums in the low-energy range. However, it was not clear whether the accuracy of the analysis had improved. This was determined by investigating the peak-to-total ratios of the energy before and after the application of K-separation. The results are depicted in figure 4. The peak-to-total ratio of the energy peaks (46.5 keV, 63.3 keV, and 92.6 keV) of  $^{210}\text{Pb}$  and  $^{234}\text{Th}$  in the

spectrum before and after K-separation was calculated, which is presented in figure 4 as illustrated in the graphs, the peak-to-the total ratio of the sample with K-separation was greater than that of the sample without K-separation. This finding proves that K-separation enhances the accuracy of the activity analysis of  $^{210}\text{Pb}$  and  $^{232}\text{Th}$  (both sensitivity and statistical uncertainty).

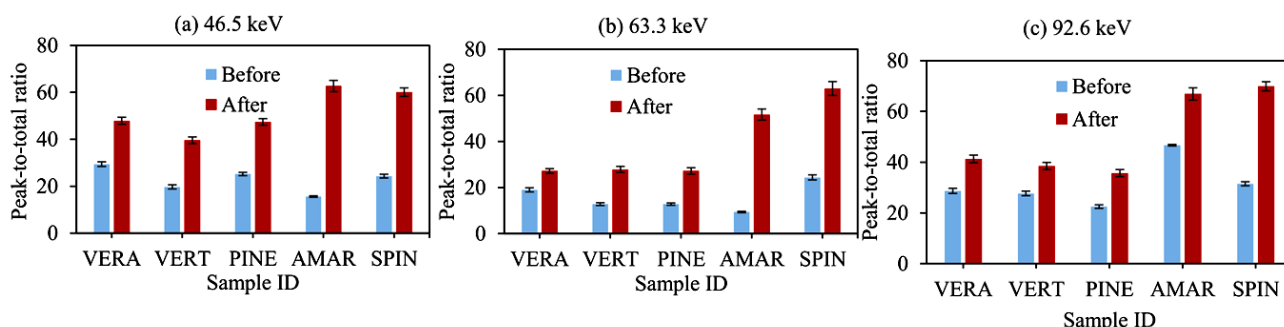


**Figure 4.** Comparison of the peak-to-total ratios of the low-energy peaks before and after K-separation: (a) 46.5 keV of  $^{210}\text{Pb}$ , (b) 63.3 keV of  $^{232}\text{Th}$ , and (c) 92.6 keV of  $^{232}\text{Th}$ .

At energy < 1000 keV, the energy peaks of the isotopes of interest included 46.5 keV of  $^{210}\text{Pb}$ , 63.3 and 92.6 keV of  $^{234}\text{Th}$ , 186.2 keV of  $^{226}\text{Ra}$ , 238.6 keV of  $^{212}\text{Pb}$ , and 338.3 and 911.1 keV of  $^{228}\text{Ac}$ . Figure 5 shows the results of activity concentrations of  $^{210}\text{Pb}$ ,  $^{238}\text{U}$ ,  $^{226}\text{Ra}$ , and  $^{212}\text{Pb}$  in AMAR, VERA, PINE, VERT,

and SPIN before and after K-separation. Some differences were observed in the values; for instance, the activity concentrations of  $^{238}\text{U}$  in the PINE sample.

To establish the reliability of the method of K-separation, the MDA values obtained using the technique were compared with the original values.



The results are presented in figure 6, which indicate that the MDA values were reduced after the  $^{40}\text{K}$ -separation. The MDA values before K-separation for 63.3 keV were in the range of 17.1–24.6 Bq/kg, whereas those after the separation were in the range of 7.0–16.4 Bq/kg. However, the deviations in MDA

values before and after the separation were different for each sample and each energy peak. Table 1 lists the deviations (%) in MDA values before and after the separation for each sample and each energy peak, thereby providing an idea of the differences in the values before and after K-separation.

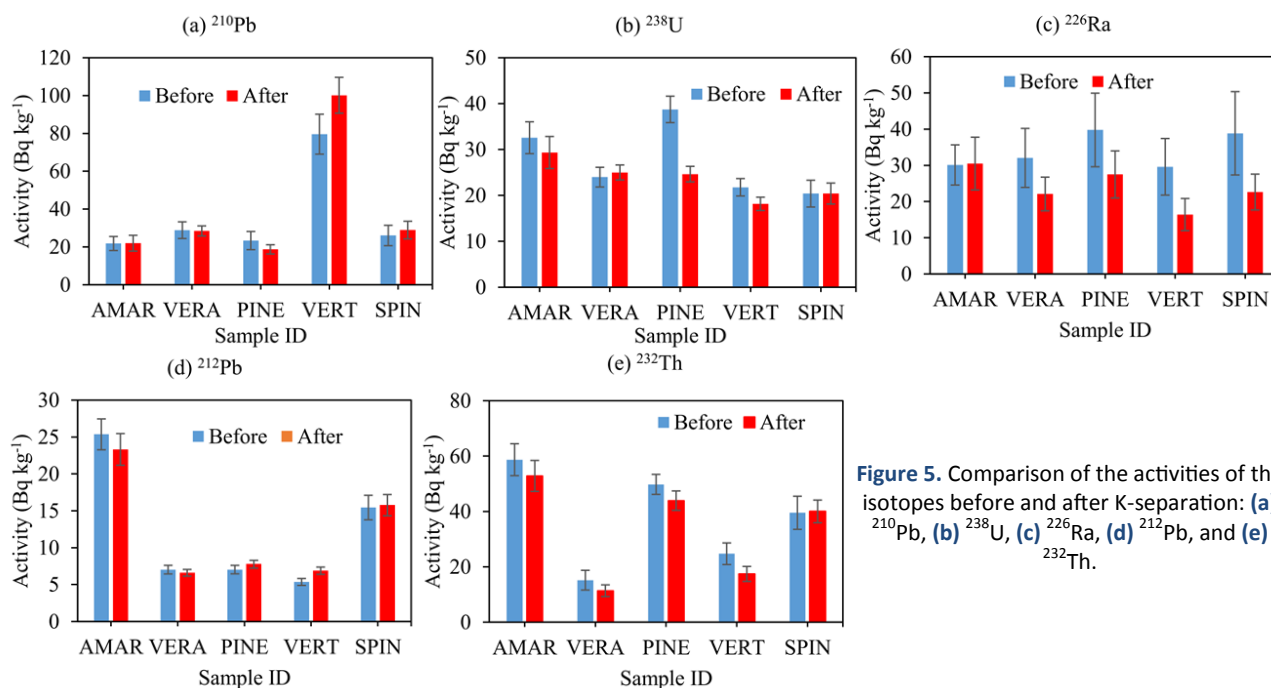


**Figure 5.** Comparison of the activities of the isotopes before and after K-separation: (a)  $^{210}\text{Pb}$ , (b)  $^{238}\text{U}$ , (c)  $^{226}\text{Ra}$ , (d)  $^{212}\text{Pb}$ , and (e)  $^{232}\text{Th}$ .

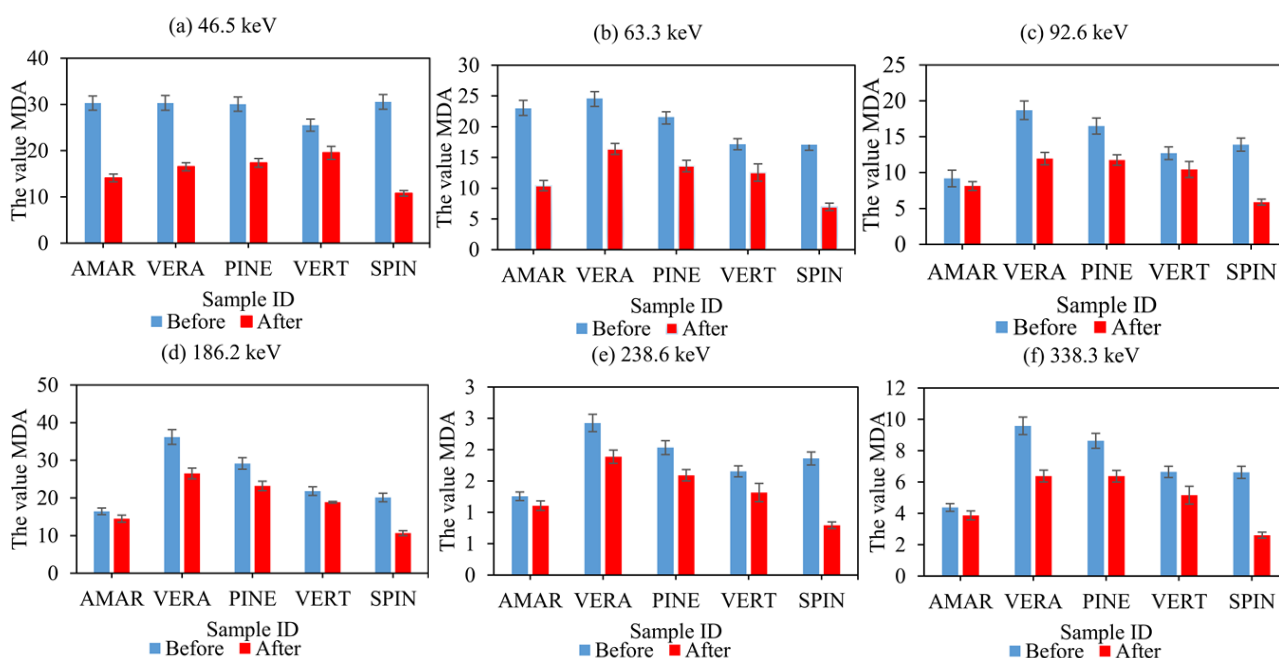


**Figure 6.** Comparison of the MDA values before and after K-separation for different gamma energies impacted by the  $^{40}\text{K}$  Compton region: (a) 46.5 keV, (b) 63.3 keV, (c) 92.6 keV, (d) 186.2 keV, (e) 238.6 keV, and (f) 338.3 keV.

**Table 1.** Deviations in MDA values before and after K-separation for each sample and each energy peak (%)  
E (keV) Activity concentration of <sup>40</sup>K (Bq kg<sup>-1</sup>)

	4700 (VERA)	5600 (PINE)	6200 (VERT)	7800 (AMAR)	9600 (SPIN)
46.5	46 (11)	42 (10)	23 (12)	53 (11)	65 (10)
63.3	33 (11)	37 (10)	27 (13)	55 (10)	59 (11)
92.6	36 (11)	29 (10)	18 (13)	11 (11)	58 (11)
186.2	27 (11)	21 (11)	14 (7)	12 (12)	47 (12)
238.6	22 (11)	22 (11)	20 (15)	12 (12)	57 (12)
338.3	33 (12)	26 (11)	22 (15)	12 (13)	61 (12)
911.1	35 (13)	43 (13)	28 (16)	22 (14)	58 (12)

## DISCUSSION

The average efficiency of <sup>40</sup>K extraction obtained from measurements of the five samples was > 90%, which is sufficient to significantly reduce the Compton continuum of <sup>40</sup>K in the measured spectrum. The complex procedure proposed by Inoue *et al.* (2003) could extract 98% of <sup>40</sup>K from seaweed samples (24). The researchers found that the high efficiency of <sup>40</sup>K extraction can improve the spectroscopic detection limit. Moreover, measurement of the leachate after the separation did not result in the detection of any other natural radionuclides. The graphs in figure 2 show that the separation process did not remove all potassium from the sample as a <sup>40</sup>K energy peak appeared in the spectrum. However, after K-separation, the counts at the energy peak of <sup>40</sup>K in the spectrum were significantly reduced (approximately 50%). In addition, the energy region of < 100 keV had a clear distinction between the spectrums (figure 2b). The area of energy below 100 keV, including the peak 46.5 keV of <sup>210</sup>Pb and 63.3 keV and 92.6 keV of <sup>234</sup>Th, was most affected by the Compton region of <sup>40</sup>K. In this region, the spectrum after K-separation displayed a lower continuum under the peaks, and the shapes of the peaks were more identifiable. In the energy range of 100–1220 keV, the background was reduced but not as remarkably as that below 100 keV, as shown in figures 2c and 2d. Figure 3 demonstrates that the sample spectrums before and after K-separation in the low-energy range of 5 – 100 keV were different. The figure further indicates that the Compton continuum under the peaks decreased and became flatter. According to the analytical results, the method of K-separation can be useful in identifying the energy peaks of radioisotopes and determining the counts on the peaks. The finding also proves that the effect of the Compton region of <sup>40</sup>K on the spectrums of other isotopes was proportional to the activity of <sup>40</sup>K in the sample.

Furthermore, the results in figure 4 signify that the peak-to-total ratio of the low-energy peaks before and after K-separation varied for different isotopes and samples. Noticeable differences were observed between the samples and energy levels. For example,

at lower energies (46.5 keV and 63.3 keV), the peak-to-total ratios differed significantly among the samples. This finding suggests that the influence of the Compton region of the <sup>40</sup>K spectrum was high, resulting in lower energy peaks and consequently lower peak-to-total ratios. The values generally showed an improvement in comparison with those before K-separation. This can be attributed to the effect of K-separation, which aids in reducing the interference and background noise, leading to better peak resolution and higher peak-to-total ratios. The peak-to-total ratio provides information on the relative strength of the specific peaks compared with the total count rate in the spectrum. A higher ratio indicates a stronger and more distinct peak relative to the background noise. Therefore, higher peak-to-total ratios imply better peak resolution and improved measurement quality. To assess the effectiveness of the method, the suppression factors (SFs) were estimated. SF is the ratio of the peak-to-total with K-separation and that without K-separation. As plotted in figure 4, the SF at the energy peak 46.5 keV varied by 62.9%, 101%, 88.1%, 300%, and 150% for VERA, VERT, PINE, AMAR, and SPIN, respectively. At 63.3 keV, the SF values were 43.2%, 118%, 118%, 450%, and 160% for VERA, VERT, PINE, AMAR, and SPIN, respectively. At 92.6 keV, the values were 40% for VERA, VERT, PINE, and AMAR and 120% for SPIN. The obtained SF values were better when compared with those from other methods of Compton suppression. The Compton suppression system employed for gamma spectrometer using experimentally validated Monte Carlo simulations significantly increased the peak-to-total ratio to 70% in the energy range of 358–382 keV (25). A digital pulse shape analysis of Compton suppression for a germanium detector could increase the peak-to-total ratio of <sup>137</sup>Cs (662 keV) from 0.206 to 0.509 (SF = 247%) (26).

For samples with K-separation, the results of the activities of the isotopes and their MDA values are presented in figure 5 and figure 6, respectively. The figures illustrate that the activities of <sup>40</sup>K were higher than those of other radioisotopes in the samples. These results agree with those from other studies (27-30). Some activity results were not acceptable because the values were lower than those of the respective MDA, namely <sup>210</sup>Pb in VERA; <sup>226</sup>Ra in VERA, PINE, and VERT; and <sup>238</sup>U in PINE and AMAR. The findings further indicate that the activity results were acceptable because all values were higher than those of the respective MDA. A comparison of the activities of the isotopes before and after applying the method showed the impact of K-separation on the measured activities. In general, after K-separation, the activities of most isotopes appeared to be lower than those before K-separation. This finding indicates that K-separation effectively reduces interference and background noise, leading to more accurate and

reliable activity measurements.

Additionally, the MDA values for the respective isotopes before and after K-separation are provided in figure 6. The MDA ratio (MR) is the ratio of MDA with K-separation and that without K-separation. For all samples and energies, the MR values were < 100% (40%–83%). This proves that the MDA was improved by the application of K-separation. Upon applying the algorithms for background subtraction in a gamma-ray spectrum, the MR values were 38% for the energy 46.5 keV of  $^{210}\text{Po}$  and 12% for the energy 662 keV of  $^{137}\text{Cs}$  (30). Done and Loan (2016) used three different MDA algorithms to reduce the Compton continuum for gamma spectrometry measurements. After applying the methods, the MDA values decreased to 1.5 (MR value approximately 66.6%) (31). The MDA represents the minimum level of activity that can be reliably detected above the background noise. Lower MDA values indicate better sensitivity and detection capabilities. The comparison of the MDAs in figure 6 suggests that the values generally improved after K-separation. This implies that the separation method effectively reduces background noise, resulting in enhanced detection sensitivity.

In the analysis of environmental radioactivity using the gamma spectrometer, low-energy peaks are always difficult to determine and introduce considerable errors owing to the influence of the large background under the energy peak of interest. In many cases, low-energy peaks are used in certain analyses, and the results are forced to accept large errors. Several previous studies have established that the suppression of the Compton continuum can increase the detection limit of the spectroscopy and improve the accuracy of the radioactivity analysis (32,33). The  $^{40}\text{K}$  Compton continuum contributes immensely to the Compton region of the spectrum. Therefore, the separation of  $^{40}\text{K}$  from the sample can significantly improve the accuracy of the analysis of these energy peaks. Based on the analysis of the deviations in table 1, it could be inferred that the deviations after separation were lower than those before separation for some samples and energy peaks. This result suggests that the separation method successfully reduced background noise and improved the accuracy of activity measurements.

For each sample, the deviation of MDA values was significantly high for energy peaks in the energy range of < 100 keV. This means that after  $^{40}\text{K}$  removal, the energy peaks can be quickly identified and calculated. Especially, the effects were clear for the activity analysis of  $^{210}\text{Pb}$  (via the energy peak 46.5 keV) and  $^{238}\text{U}$  (via the energy peaks 63.3 keV and 92.6 keV of  $^{234}\text{Th}$ ). According to the results, maximum MDA deviation was observed for the water spinach sample, whereas the minimum value was noted for the vetiver grass sample. These observations indicate that the  $^{40}\text{K}$ -separation is an

effective method to improve the analytical accuracy of some natural radioisotopes.

## CONCLUSION

During environmental radioactivity analysis using a gamma spectrometer, the Compton continuum of  $^{40}\text{K}$  covers the energy peaks of some radionuclides, especially the energy regions between 0 keV and 100 keV. Therefore, it is necessary to identify an effective method to remove  $^{40}\text{K}$  from the samples. The simple chemical procedure used in this study could extract > 90% potassium from the biota samples. Upon applying this method, the peak-to-total ratio increased approximately 1.5 times in the energy range of 0–100 keV of the spectrum. In addition, the MDA values of the measurements improved significantly, decreasing from  $24.6 \text{ Bq kg}^{-1}$  to  $16.4 \text{ Bq kg}^{-1}$ .

## ACKNOWLEDGMENTS

*The authors would like to thank the reviewers, English proofreaders and editors for their thorough review and highly appreciated comments and suggestions, which significantly contributed to improving the quality of this manuscript.*

**Funding:** This research is funded by University of Science, VNU-HCM under grant number T2022-43.

**Conflicts of interests:** The authors declare no competing interests.

**Ethical consideration:** Not applicable.

**Author contribution:** Truong Huu Ngan Thy, Huynh Thi Yen Hong: Sample collection; Radioactivity analysis. Truong Huu Ngan Thy, Nguyen Van Thang; Manuscript preparation; Data analysis. Trinh Hoa Lang, Le Cong Hao: Review the manuscript; Supervisor.

## REFERENCES

- Knoll GF (2010) Radiation detection and measurement. 4th ed. New York, NY: John Wiley & Sons.
- Zehring MR (2017) Gamma-Ray Spectrometry and the Investigation of Environmental and Food Samples, *New Insights on Gamma Rays*. Intech Open.
- Buchtela K (2019) Radiochemical methods | Gamma-Ray Spectrometry, Encyclopedia of Analytical Science (Third Edition), Academic Press.
- Radulescu I, Blebea-Apostu AM, Margineanu RM, et al. (2013) Background radiation reduction for a high-resolution gamma-ray spectrometer used for environmental radioactivity measurements. *Nucl Instrum Methods Phys Res A* **715**: 112–118.
- Canberra Industries (2004) Genie 2000 version 30—customization tools manual. *Canberra Industries Inc., Meriden*.
- Chinnaesakki S, Bara SV, Sartandel SJ, et al. (2012) Performance of HPGe gamma spectrometry system for the measurement of low level radioactivity. *J Radioanal Nucl Chem* **294**: 143–147.
- Moiseev DV and Lukina LI (2020) Improving the accuracy of gamma radiation measurements in radiation monitoring. *IOP Conf Ser: Earth Environ Sci* **548**: 032009.
- Gawad KAE, Zhang Z, Hazza MH (2020) Improving the analysis performance of gamma spectrometer using the Monte Carlo code for

- accurate measurements of uranium samples, *Results Physics* **17**: 103145.
9. Manolopoulou M, Stoulos S, Mironaki D, Papastefanou C (2003) A new technique for the accurate measurement of  $^{226}\text{Ra}$  by gamma spectroscopy in voluminous samples. *Nucl Instrum Methods Phys Res A* **508**: 362–366.
  10. British Standard (2005) Measurement of radioactivity in the environment—Soil. *BS ISO 18589-1*: 2005.
  11. Jelena NP, Deborah HO, Brit S (2020) Transfer of naturally occurring radionuclides from soil to wild forest flora in an area with enhanced legacy and natural radioactivity in Norway. *Environ Sci: Processes Impacts* **22**: 350–363.
  12. Nguyen TD, Duong VH, Bui VL, et al. (2021) Natural radionuclides and assessment of radiological hazards in Muong Hum, Lao Cai, Vietnam. *Chemosphere* **270**: 128671.
  13. Perevoshchikov R, Perminova A, Menshikova E (2022) Natural Radionuclides in Soils of Natural-Technogenic Landscapes in the Impact Zone of Potassium Salt Mining. *Minerals* **12**: 1352.
  14. Polaczek-Grelak K, Kisiel J, Walencik-tata A, et al. (2016) Lead shielding efficiency from the gamma background measurements in the salt cavern of the Polkowice–Sieroszowice copper mine. *J Radioanal Nucl Chem* **308**: 773–780.
  15. Ali MDM, Eisa MEM, Mars JA (2021) Study of gamma rays shielding parameters of some building materials used in Sudan. *Int J Radiat Res* **19(1)**: 191–196.
  16. Alghamdi AS, Aleissa KA (2015) Ultra-low-background gamma spectroscopy for the measurement of environmental samples. *J Radioanal Nucl Chem* **303**: 479–484.
  17. Thiesse M, Scovell P, Thompson L (2022) Background shielding by dense samples in low-level gamma spectrometry. *Appl Radiat Iso* **188**: 110384.
  18. Mitra MS, Sarkar PK (2005) Monte Carlo simulations to estimate the background spectrum in a shielded NaI(Tl)  $\gamma$ -spectrometric system. *Appl Radiat Iso* **63**: 415–422.
  19. Li S, Wang L, Cheng Y, et al. (2016) A novel natural environment background model for Monte Carlo simulation and its application in the simulation of anticoincidence measurement. *Appl Radiat Iso* **108**: 75–81.
  20. Riyadh M, Al-Hamzawi AA (2023) Natural radionuclides and radiological hazards in sediment samples of the Euphrates River in Al Diwaniyah governorate, Iraq. *Int J Radiat Res* **21(1)**: 159–162.
  21. Eke BC, Ukewuihe UM, Akomolafe IR (2022) Evaluation of activity concentration of natural radionuclides and lifetime cancer risk in soil samples at two tertiary institutions in Owerri, Imo State, Nigeria. *Int J Radiat Res* **20(3)**: 671–678.
  22. Onjefu SA, Johannes NN, Abah J, et al. (2022) Natural radioactivity levels and evaluation of radiological hazards in Usakos marble, Erongo region, Namibia. *Int J Radiat Res* **20(2)**: 403–409.
  23. Arnold D, Debertin K, Heckel A, et al. (2018) Fundamentals of gamma spectrometry. Federal Ministry for Environment, *Nature Conservation and Nuclear Safety (Germany)*.
  24. Inoue M, Kofuji H, Yamamoto M, et al. (2003) Application of low background gamma-ray spectrometry to environmental monitoring samples: Water leaching treatment for  $^{40}\text{K}$ -removal. *J Radioanal Nucl Chem* **255**: 211–215.
  25. Scates W, Hartwell JK, Aryaeinejad R, McIlwain ME (2006) Optimization studies of a Compton suppression spectrometer using experimentally validated Monte Carlo simulations. *Nucl Instrum Methods Phys Res A* **556**: 498–504.
  26. Jung HS, Cho HY, Lee JH, Lee CS (2007) Improvement of the Compton suppression ratio of a standard BGO suppressor system by a digital pulse shape analysis. *Nucl Instrum Methods Phys Res A* **580**: 1016–1019.
  27. Changizi V, Jafarpour Z, Naseri M (2010) Measurement of  $^{226}\text{Ra}$ ,  $^{228}\text{Ra}$ ,  $^{137}\text{Cs}$  and  $^{40}\text{K}$  in edible parts of two types of leafy vegetables cultivated in Tehran Province-Iran and resultant annual ingestion radiation dose. *Iran. J. Radiat. Res.* **8**: 103–110.
  28. Oyekunle JAO, Ogundele KT, Adekunle AS, et al. (2019) An Assessment of Radiological Hazard Levels in Vegetables and Condiments Obtained from Ile-Ife Main Market, Ile-Ife, *Nigeria Inter J Sci Res Pubs (IJSRP)* **9(6)**: p90105.
  29. Robison WL, Hamilton TF, Conrado CL, et al. (2006) Uptake of Cesium-137 by leafy vegetables and grains from calcareous soils. Lawrence Livermore National Laboratory, Livermore, CA, *United States of America, IAEA-TECDOC-1497*.
  30. Saeed MA, Wahab NAA, Hossain I, et al. (2011) Measuring radioactivity level in various types of rice using hyper pure germanium. *Inter J Phys Sci* **6**: 7335 – 7340.
  31. Tomarchio E, Giardina M, Buffa, P (2023) A baseline estimation procedure to improve MDA evaluation in gamma-ray spectrometry. *Eur Phys J Plus* **138**: 700.
  32. Done L, Loan MR (2016) Minimum Detectable Activity in gamma spectrometry and its use in low level activity measurements. *Appl Radiat Iso* **114**: 28–32.
  33. Scates W, Hartwell JK, Aryaeinejad R, et al. (2006) Optimization studies of a Compton suppression spectrometer using experimentally validated Monte Carlo simulations. *Nucl Inst Meth Phys Res A* **556**: 498–504.
  34. Cai SL, Cai X, Wu ZZ, et al. (2015) Simulation of background reduction and Compton suppression in a low-background HPGe spectrometer at a surface laboratory. *Chinese Phys. C* **39** 086002.